Experimental study of Coulomb corrections and single-particle energies for single-walled carbon nanotubes using cross-polarized photoluminescence

K.-C. Chuang (莊凱捷),[1] A. Nish,[1] J.-Y. Hwang (黃炯源),[2] G. W. Evans,[1] and R. J. Nicholas[1]
[1]*Department of Physics, Oxford University, Clarendon Laboratory, Parks Road, Oxford OX1 3PU, United Kingdom*
[2]*Department of Material Science and Engineering and Centre for Condensed Matter Sciences, National Taiwan University, Taipei, 106 Taiwan*

(Received 25 February 2008; revised manuscript received 18 April 2008; published 12 August 2008)

We report the observation of cross-polarized transitions of single-walled carbon nanotubes (SWCNTs) isolated with aromatic polymers. The use of photoluminescence excitation mapping allows the identification of the transitions of individual species of SWCNT. Comparing experimental observation with theory yields an estimate for the Coulomb interactions, which is dependent on the nanotubes' diameter and environment. Values for the single-particle energies are deduced and found to be in good agreement with the predictions of tight-binding models.

DOI: 10.1103/PhysRevB.78.085411 PACS number(s): 78.67.Ch, 78.55.−m, 81.07.De

Single-walled carbon nanotubes (SWCNTs) display remarkable electronic and mechanical properties, such as high mobility one-dimensional (1D) transport and high mechanical and thermal stability,[1] and they have attracted enormous interest across several research fields. The electronic properties of SWCNTs depend critically on the structure of the nanotubes,[2] defined by the chiral indices n and m. Detailed studies of the optical properties of nanotubes have been made possible by the successful isolation of SWCNTs using surfactant wrapping techniques, which allow the observation of photoluminescence (PL) from semiconducting SWCNTs.[3] PL spectroscopy, in conjunction with photoluminescence excitation (PLE) spectroscopy, allows the identification of the first and second van Hove optical transitions (E_{11} and E_{22}) for individual nanotube species. Over the past few years, PLE mapping has not only become an important tool for measuring nanotube transition energies[4–7] and characterization[8–10] but also for understanding the role of many body interactions,[11–13] which strongly affect the optical properties of SWCNTs. The theoretical properties of excitons have long been predicted[14,15] and are very significant owing to the one-dimensional nature of the nanotubes. This was recently confirmed by two photon absorption experiments.[11,12] However, the full Coulomb interaction picture is more complex as pointed out by Ando *et al.*[14] who showed that electron-electron interactions are larger than the electron-hole coupling of the excitons and the total Coulomb interaction needs to be considered when describing the electronic transitions of SWCNTs.

Advances in sample preparation techniques such as multiple density gradient ultracentrifugation[16] and the use of DNA (Ref. 17) as a dispersive agent, as well as suspending SWCNTs over trenches,[18] are now allowing PL observations for single species of SWCNTs. A particularly effective method has recently been reported, using highly selective aromatic polymers with a variety of different solvents[19,20] to disperse SWCNTs. These solutions contain far fewer nanotube species and fewer impurities compared to the surfactant wrapped samples and are also simple to prepare. As a result it is possible to identify a number of weaker features in the PLE spectra, which would otherwise be overwhelmed by PL signals from other nanotube species. By using different combinations of starting material, polymer and solvent, detailed studies of PLE spectra can be performed for a range of different SWCNT species.

In this paper, we report a study of the E_{11}, E_{22}, and in particular a perpendicular polarized optical transitions assigned to E_{12}, which allow us to deduce the magnitude of the Coulomb interaction effects. This perpendicularly polarized transition is weak and was first observed only recently.[21,22] It is allowed by interband selection rules and is observed most strongly for light polarized perpendicular to the tube axis, where it is least suppressed due to depolarization effects.[23] This transverse transition originates when an electron absorbs a photon, which excites it from the first (second) valence band to the second (first) conduction band leaving a hole behind. The electron (hole) then decays nonradiatively to the first conduction (valence) band where recombination happens, emitting a photon of energy E_{11}. The Coulomb interactions influence the transition energies for both the absorption and emission processes. In a simple single-particle picture, assuming electron-hole symmetry, these two transitions would be identical, situated in the middle of E_{11} and E_{22} given by $(E_{11}+E_{22})/2$. In practice, however, a small asymmetry exists between the conduction and valence band, possibly causing a splitting between the two transitions.[1,24] Furthermore, electron-electron interactions mix these two states, creating a weak dipole-forbidden transition, which is redshifted with respect to the central state, and a dominant dipole-allowed transition (E_{12}), which is blueshifted[25] and is measured here. This blueshift was calculated by Uryu *et al.*[26] for all three transitions, and using their theory the strength of the Coulomb interactions can then be compared with experiment.

The polymers used in this study were poly[9,9-dioctylfluorenyl-2,7-diyl] (PFO), poly[9,9-dioctylfluorenyl-2,7-diyl)-alt-co-(1,4-benzo-2,1',3-thiadiazole)] (PFO-BT), and poly[(9,9-dioctylfluorenyl-2,7-diyl)-co-(1,4-phenylene)] (PFO-P) purchased from American Dye Source Inc. SWCNTs grown by both HiPCO and CoMoCAT processes were purchased from Carbon Nanotech. and Southwest Nanotech., respectively. Laser vaporization grown samples

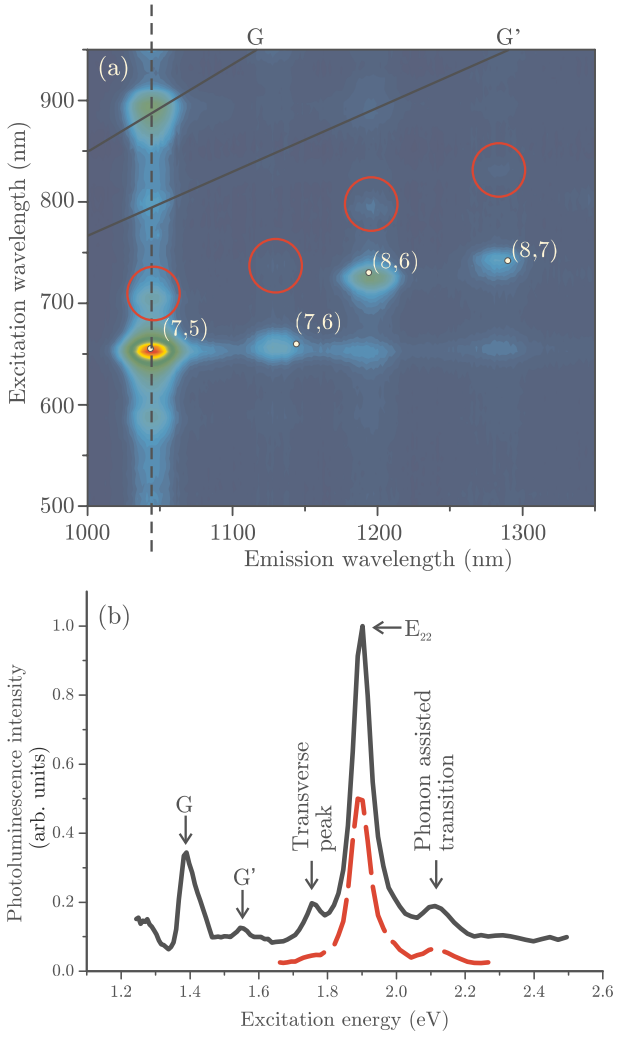

FIG. 1. (Color online) (a) PLE map of CoMoCAT nanotubes wrapped by PFO in o-xylene with only four nanotube species observed. Species are determined by using a semiempirical model (Ref. 27). The circles identify E_{12} transitions associated with each species of nanotube. Clear resonant Raman features associated with the G and G' band can also be observed. (b) PLE spectrum of (7,5) nanotube species. This spectrum is taken from a vertical slice of the PLE map, indicated by the black (dotted) line in Fig. 1(a). The intensity is normalized to the main peak, which corresponds to the E_{22} transition, while several other smaller features are also observed and identified. The red (dashed) line corresponds to parallel polarized PLE spectra of the same species with the intensity decreased in absolute terms by a factor of seven for clarity. The transverse peak feature is much weaker in this spectrum.

were provided by Björn Hornbostel of the Max-Planck-Institut für Festkörperforschung, Stuttgart. The solvents used were o-xylene and toluene. The nanotubes were dispersed in solutions in the ratio 5 mg SWCNTs:6 mg polymer:10 ml solvent. Surfactant wrapped nanotubes were prepared by adding 20 mg of nanotubes to 1 wt% sodium dodecylbenzene sulfonate (SDBS) in D_2O, sonicated for 30 min then ultracentrifuged for 4 h. PLE mapping was carried out using an automated custom built system consisting of a 75 W xenon lamp focused into a monochromator, which then illuminated the sample in a quartz fluorescence cell using a 5-nm wavelength steps. The photon flux was normalized using a silicon photodiode. Luminescence from the sample was collected at 90° to the excitation beam and focused into a spectrograph fitted with a liquid nitrogen cooled 512 element InGaAs photodiode array. Polarized PLE spectra were taken with both the excitation and emission light, appropriately polarized.

TABLE I. Table showing E_{11}, E_{12}, and E_{22} transition energies for the different nanotube species observed, as obtained by fitting the spectra with a commercial peak fitting program.

Nanotube species	Diameter (nm)	E_{11} (eV)	E_{12} (eV)	E_{22} (eV)
(6,5)	0.757	1.24	1.90	2.15
(8,7)	1.032	0.97	1.50	1.67
(9,7)	1.103	0.92	1.40	1.55
(8,6)	0.966	1.04	1.56	1.71
(7,5)	0.829	1.19	1.76	1.90
(9,8)	1.169	0.87	1.35	1.51
(7,6)	0.895	1.10	1.68	1.89
(10,5)	1.050	0.98	1.45	1.56
(9,4)	0.916	1.10	1.59	1.70

An example of a PLE false color contour map is presented in Fig. 1(a) for the cross-polarized configuration, and a PLE spectrum of a (7,5) nanotube, corresponding to a vertical slice of the contour plot represented by the black dotted line, are shown in Fig. 1(b). As well as the prominent E_{22} resonant feature, several weaker features such as phonon-assisted transitions and resonant Raman features can be seen in Fig. 1(b). The main point of interest, however, is the feature labeled as the transverse peak, which corresponds to preferential absorption of light perpendicular to the nanotube axis, as expected for E_{12}. This feature is almost entirely absent if the emitted light is of the same polarization as the excitation light and the spectrum is dominated by the stronger E_{22} transition, as demonstrated by the red graph in Fig. 1(b). Thus confirming that the E_{12} feature is due to transverse excitation. In contrast to the results of Miyauchi *et al.*[21] (where two transverse peaks are seen) only one transverse peak is observed, consistent with the model of Zhao *et al.*[25] and the results of Lefebvre *et al.*[22] We therefore label this peak E_{12}, which we were able to observe for a total of nine nanotube species using different combinations of nanotube samples and polymers, with a summary of data given in Table I. The relative magnitude of the E_{12} peak ($\sim$10% of E_{22}) is, however, still small compared to the results of Lefebvre *et al.*[22] due to the random orientation of the nanotubes, which means that even in the crossed polarization the dominant contribution to the absorption comes from E_{22} and other parallel polarization allowed transitions for tubes that are not oriented along either of the polarization directions.

Figure 2(a) shows the relation between E_{12} and the values of $(E_{11}+E_{22})/2$. This shows that E_{12} is systematically blueshifted—in agreement with the calculations of Uryu *et al.*,[26] which predict that the relative magnitude of the electron-electron contribution to E_{12} is significantly larger

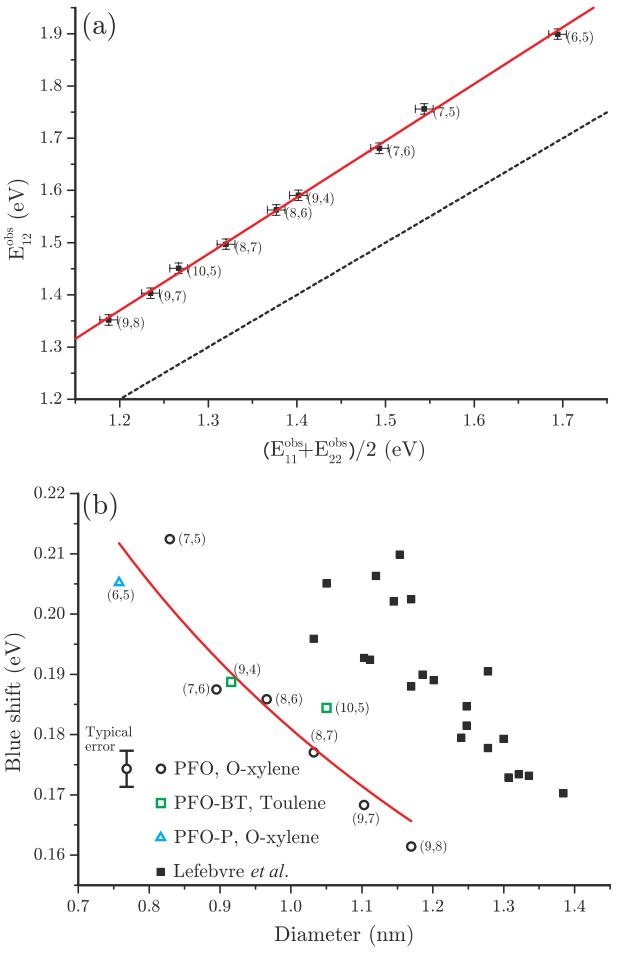

FIG. 2. (Color online) (a) Plot of E_{12}^{obs} against $(E_{11}^{obs}+E_{22}^{obs})/2$. The red (solid) line indicates linear best fit and the black (dashed) line indicates $E_{12}^{obs}=(E_{11}^{obs}+E_{22}^{obs})/2$. (b) Blueshift ΔE against the diameter for polymer wrapped species (hollow points) with $\Delta E = Ax^{-B}$, with $A=0.18$ and $B=0.57$. Results for air suspended nanotubes from the work of Lefebvre *et al.* (Ref. 22) are shown as full squares.

than for E_{11} and E_{22}. The blueshift $\Delta E=E_{12}-(E_{11}+E_{22})/2$ increases as the diameter of the nanotube decreases. Fitting this to a power-law dependence on nanotube diameter gives $\Delta E=Ad^{-B}$, with $A=0.18$ and $B=0.57$.

To analyze the relationship between blueshift and Coulomb interactions further, we first write

$$E_{11}^{obs} = E_{11}^{gap} + \delta_{11},$$

$$E_{22}^{obs} = E_{22}^{gap} + \delta_{22},$$

$$E_{12}^{obs} = E_{12}^{gap} + \delta_{12},$$

$$E_{12}^{gap} = \frac{(E_{11}^{gap} + E_{22}^{gap})}{2},$$

where E^{obs} indicates the experimental values, E^{gap} is the true band-gap value of the transition energy in the noninteracting picture, and δ is the correction from the Coulomb interactions. In this nomenclature, the blueshift, ΔE, is equal to $\delta_{12}-\frac{\delta_{11}+\delta_{22}}{2}$, which is purely dependent on the Coulomb interactions, thus allowing us to remove the majority of band-structure effects such as the family shifts of the single-particle energies.[28] By fitting our blueshift values to the calculations reported by Uryu *et al.*,[26] we extract the magnitude of the Coulomb interaction parameter—expected to be of order $\frac{e^2}{4\pi^2\epsilon\epsilon_0 d}$ $(0.458/\epsilon$ eV for a 1 nm tube)—for each of the nanotube species. The value for γ_0 needed for the conversion from the dimensionless units used in Uryu and Ando's model is taken to be 2.75 eV from the tight-binding models discussed below.[28,29] The fitting gave values for the Coulomb interaction parameter ranging from 0.122 to 0.155 eV, dependent on the diameter of the tubes. Using the same analysis procedure on the experimental results of Lefebvre *et al.*[22] (where PLE spectra were taken for a different set of SWCNTs suspended in air), there is a global increase of ~20% in the strength of Coulomb interactions, as shown in Fig. 3(a). Fitting the two sets of data to a power-law dependence on diameter gives $E_c=Cd^{-D}$, with $C=0.134$ and 0.163 for $D=0.55$, giving a similar power-law dependence to that observed for the directly measured blueshift ΔE. It should be noted however that there is still evidence of a significant dependence upon chiral angle, which is particularly noticeable in the data of Lefebvre *et al.*[22] due to their observation of considerably more nanotube species with small chiral angles. Such an effect is to be expected due to the presence of trigonal warping, which will influence parameters such as the effective mass (which will alter the magnitude of the Coulomb interactions).[30] The overall differences in the Coulomb interactions between our data and the experimental results of Lefebvre *et al.*[22] are caused by the higher dielectric constant of the surrounding medium (compared to vacuum), which therefore produces a shift to lower energies due to the dominance of the electron-electron interactions. Scaling behavior has been calculated for both the exciton binding energy alone with Perebeinos *et al.*[31] predicting $E_b \sim \epsilon^{-1.4}d^{-1}$ and the calculations for all of the Coulomb terms,[32] which suggest a scaling dependence with $E_b \sim d^{-1}$ (which may be reduced by the inclusion of a logarithmic correction). Our data show that the diameter dependence of the Coulomb effects is less than predicted by the simple scaling laws, in agreement with previous suggestions,[33] but that family effects may be larger than predicted[30] and large enough to influence the Coulomb energy even for the lowest-energy bands.

Using our detailed fitting of the magnitude of the Coulomb interactions it is then possible to deduce the single-particle band-gap energies for a large range of nanotubes. In order to extend the range of species for which we can deduce the single-particle energies we also include an analysis of the PLE spectra for nanotubes dispersed in aqueous suspensions using the SDBS, which is much less selective. The Coulomb interactions for SDBS solution have the factor C adjusted to be $C=0.148$, which produces consistent band gaps for the species that are observed in common for all three sets of data.

The above procedure allowed us to deduce the values for the single-particle band gaps shown in Fig. 3(b), which can then be compared with theory. This is a significant result as

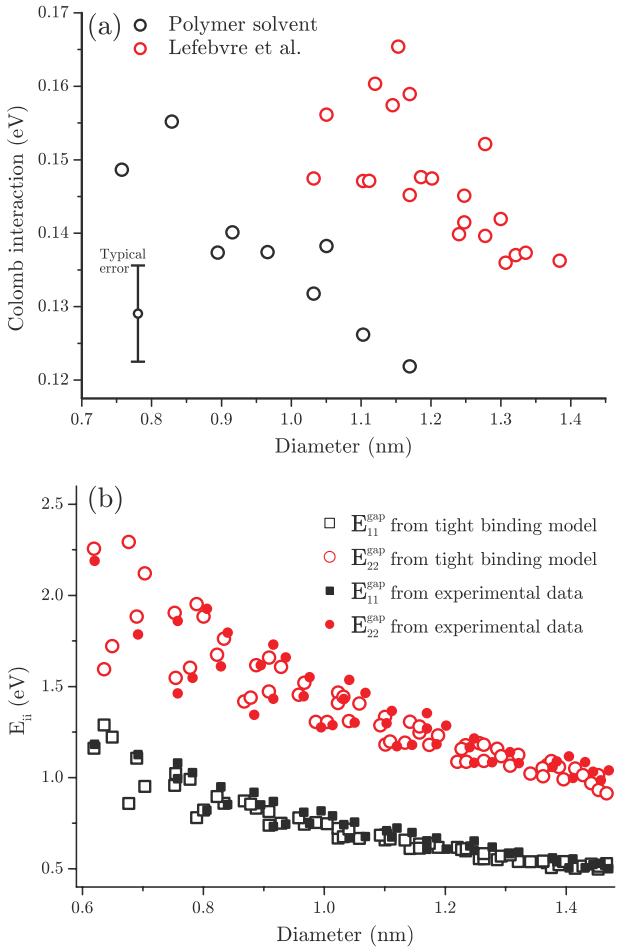

FIG. 3. (Color online) (a) Plot of Coulomb interaction energy against the diameter of SWCNTs. The strength of the Coulomb interactions is greater for nanotubes suspended in air than in solvent isolated by polymers. (b) Comparison of experimental (solid symbols) and theoretical (open symbols) single-particle E_{ii}^{gap} as a function of nanotube diameter. The experimental values were deduced using measurements with both SDBS and polymer wrapped nanotubes. The theoretical results are from the tight-binding model developed by Popov *et al.* (Ref. 29).

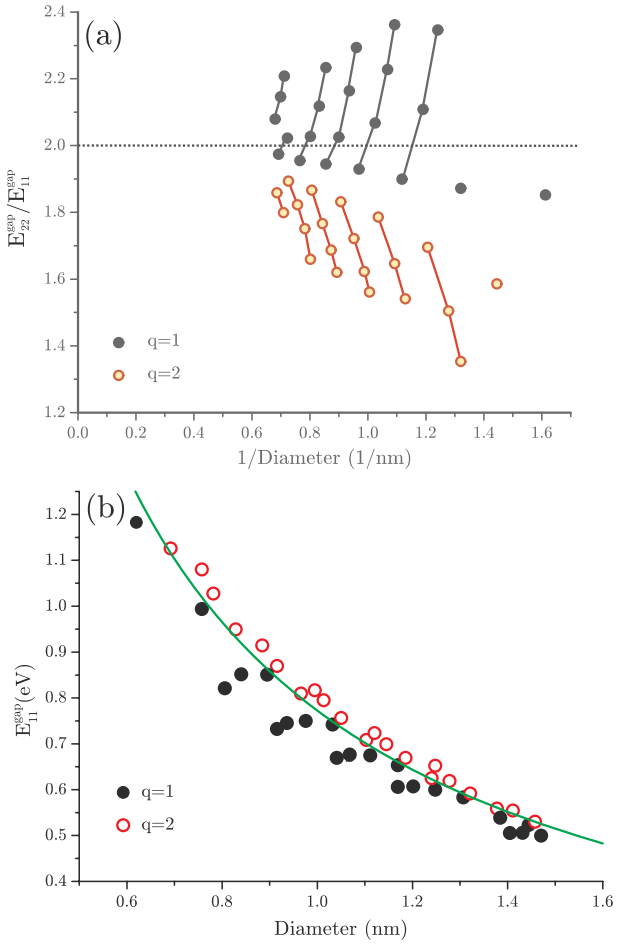

FIG. 4. (Color online) (a) A plot of the ratio $E_{22}^{gap}/E_{11}^{gap}$ for the experimental single-particle gaps shown in Fig. 3(b) as a function of diameter. The chiral index q is given by $n-m=3p+q$, where p is an integer. (b) E_{11}^{gap} deduced from the SDBS wrapped nanotube data. The green (solid) line shows the band gap as predicted from a linear dispersion, $E_g=4\hbar c/3d$, with $c=0.88\times10^6$ ms^{-1}.

previous attempts to measure single-particle gaps from scanning tunneling microscopy (STM) are not particularly accurate and have suggested a range of γ_0 from 2.45 to 2.8 eV,[34–36] while careful analysis of resonance Raman experiments still do not provide independent values of the single-particle band gaps and hence of γ_0.[37–41] Our single-particle values are compared with the symmetry adapted nonorthogonal tight-binding model developed by Popov,[28,29] which is based on the assumption of a value for $\gamma_0=2.75$ eV. The agreement is excellent with only small differences for the smallest diameter tubes.

An interesting comparison with simple theory can be seen by plotting the ratio of $E_{22}^{gap}/E_{11}^{gap}$, as shown in Fig. 4. It can be seen here that this ratio does approach the expected value of two, for nanotubes close to the armchair configuration, but only in the limit of large nanotube diameter where the graphene dispersion relation becomes linear. The deviation away from two for smaller nanotubes is caused by the combination of curvature and trigonal warping effects in the band structure.[9] In the large diameter limit Fig. 4(b) shows that the nanotube band gaps tend toward the linear dispersion result $E_g=4\hbar c/3d$ with a value of $c=0.88\times10^6$ ms^{-1}, where $c=\frac{\sqrt{3}}{2}\frac{\gamma_0 a_0}{\hbar}$ corresponding to a value of $\gamma_0=2.72$ eV. These values are over 20% lower than the recently measured values for c in monolayer graphene,[42,43] which are of order 1.1×10^6 as measured by cyclotron resonance, and are consistent with the picture suggested by Chuang *et al.*[44] that there is a systematic decrease in values of c and γ_0 from graphene to carbon nanotubes with a few layer turbostratic graphene giving intermediate values.[45]

In summary, using aromatic polymer wrapped SWCNTs in solvents, we were able to measure PLE spectra for several different species of nanotubes. The transverse transitions are successfully identified and found to be blueshifted significantly compared to the expected values from a single-particle picture. The observed shifts allowed us to make detailed comparisons with the predictions of theory and allowed us to measure the diameter dependence of the Coulomb interactions. This analysis also allowed us to deduce

the single-particle energies for a large range of nanotube species and demonstrate that these are in good agreement with the predictions of theory.[28]

This work was supported by the EPSRC-GB basic technology grant scheme. We would like to thank the support of C. Pears and D. W. Hsu in the provision of the ultracentrifuge facility. K.-C.C. acknowledges the financial support from the Ministry of Education, Taiwan. J.-Y.H. would like to thank the National Science Council of Taiwan and the Thousand Mile Horse Program for their financial support. G.W.E. is funded by the Nuffield foundation.

[1] R. Saito, G. Dresselhaus, and M. S. Dresselhaus, *Physical Properties of Carbon Nanotubes* (Imperial College, Singapore, 1998).
[2] R. Saito, M. Fujita, G. Dresselhaus, and M. S. Dresselhaus, Appl. Phys. Lett. **60**, 2204 (1992).
[3] M. J. O'Connell, S. M. Bachilo, C. B. Huffman, V. C. Moore, M. S. Strano, E. H. Haroz, K. L. Rialon, P. J. Boul, W. H. Noon, and C. Kittrell, Science **297**, 593 (2002).
[4] J. Lefebvre, J. M. Fraser, Y. Homma, and P. Finnie, Appl. Phys. B: Lasers Opt. **78**, 201402 (2004).
[5] R. S. Deacon, K.-C. Chuang, J. Doig, I. B. Mortimer, and R. J. Nicholas, Phys. Rev. B **74**, 201402(R) (2006).
[6] L.-J. Li, T.-W. Lin, J. Doig, I. B. Mortimer, J. G. Wiltshire, R. A. Taylor, J. Sloan, M. L. H. Green, and R. J. Nicholas, Phys. Rev. B **74**, 245418 (2006).
[7] K. Arnold, S. Lebedkin, O. Kiowski, F. Hennrich, and M. M. Kappes, Nano Lett. **4**, 2349 (2004).
[8] S. Lebedkin, F. Hennrich, T. Skipa, and M. M. Kappes, J. Phys. Chem. B **107**, 1949 (2003).
[9] S. M. Bachilo, M. S. Strano, C. Kittrell, R. H. Hauge, R. E. Smalley, and R. B. Weisman, Science **298**, 2361 (2002).
[10] S. M. Bachilo, L. Balzano, J. E. Herrera, F. Pompeo, D. E. Resasco, and R. B. Weisman, J. Am. Chem. Soc. **125**, 11186 (2003).
[11] F. Wang, G. Dukovic, L. E. Brus, and T. F. Heinz, Science **308**, 838 (2005).
[12] J. Maultzsch, R. Pomraenke, S. Reich, E. Chang, D. Prezzi, A. Ruini, E. Molinari, M. S. Strano, C. Thomsen, and C. Lienau, Phys. Rev. B **72**, 241402(R) (2005).
[13] I. B. Mortimer and R. J. Nicholas, Phys. Rev. Lett. **98**, 027404 (2007).
[14] T. Ando, J. Phys. Soc. Jpn. **73**, 3351 (2004).
[15] C. L. Kane and E. J. Mele, Phys. Rev. Lett. **90**, 207401 (2003).
[16] M. S. Arnold, A. A. Green, J. F. Hulvat, S. I. Strupp, and M. C. Hersam, Nat. Nanotechnol. **1**, 60 (2006).
[17] M. Zheng, A. Jagota, E. D. Semke, B. A. Diner, R. S. Mclean, S. R. Lustig, R. E. Richardson, and N. G. Tassi, Nat. Mater. **2**, 338 (2003).
[18] J. Lefebvre, D. G. Austing, J. Bond, and P. Finnie, Nano Lett. **6**, 1603 (2006).
[19] A. Nish, J.-Y. Hwang, J. Doig, R. J. Nicholas *et al.*, Nat. Nanotechnol. **2**, 640 (2007).
[20] J.-Y. Hwang, A. Nish, J. Doig, S. Douven, C.-W. Chen, L.-C. Chen, and R. J. Nicholas, J. Am. Chem. Soc. **130**, 3543 (2008).
[21] Y. Miyauchi, M. Oba, and S. Maruyama, Phys. Rev. B **74**, 205440 (2006).
[22] J. Lefebvre and P. Finnie, Phys. Rev. Lett. **98**, 167406 (2007).
[23] H. Ajiki and T. Ando, Jpn. J. Appl. Phys., Suppl. **34-1**, 107 (1994).
[24] A. Grüneis, R. Saito, J. Jiang, G. G. Samsonidze, M. A. Pimenta, A. Jorio, A. G. Souza Filho, G. Dresselhaus, and M. S. Dresselhaus, Chem. Phys. Lett. **387**, 301 (2004).
[25] H. Zhao and S. Mazumdar, Phys. Rev. Lett. **93**, 157402 (2004).
[26] S. Uryu and T. Ando, Phys. Rev. B **74**, 155411 (2006).
[27] R. B. Weisman and S. M. Bachilo, Nano Lett. **3**, 1235 (2003).
[28] V. N. Popov, New J. Phys. **6**, 17 (2004).
[29] V. N. Popov and L. Henrard, Phys. Rev. B **70**, 115407 (2004).
[30] K. Sato, R. Saito, J. Jiang, G. Dresselhaus, and M. S. Dresselhaus, Phys. Rev. B **76**, 195446 (2007).
[31] V. Perebeinos, J. Tersoff, and P. Avouris, Phys. Rev. Lett. **92**, 257402 (2004).
[32] C. L. Kane and E. J. Mele, Phys. Rev. Lett. **93**, 197402 (2004).
[33] A. Jorio, C. Fantini, M. A. Pimenta, R. B. Capaz, G. G. Samsonidze, G. Dresselhaus, M. S. Dresselhaus, J. Jiang, N. Kobayashi, A. Grüneis, and R. Saito, Phys. Rev. B **71**, 075401 (2005).
[34] T. W. Odom, J.-L. Huang, P. Kim, and C. M. Lieber, Nature (London) **391**, 62 (1998).
[35] J. W. G. Wildöer, L. C. Venema, A. G. Rinzler, R. E. Smalley, and C. Dekker, Nature (London) **391**, 59 (1998).
[36] M. Ouyang, J.-L. Huang, C. L. Cheung, and C. M. Lieber, Science **292**, 27 (2001).
[37] M. A. Pimenta, A. Marucci, S. A. Empedocles, M. G. Bawendi, E. B. Hanlon, A. M. Rao, P. C. Eklund, R. E. Smalley, G. Dresselhaus, and M. S. Dresselhaus, Phys. Rev. B **58**, R16016 (1998).
[38] A. G. Souza Filho, S. G. Chou, G. G. Samsonidze, G. Dresselhaus, M. S. Dresselhaus, L. An, J. Liu, A. K. Swan, M. S. Ünlü, B. B. Goldberg, A. Jorio, A. Grüneis, and R. Saito, Phys. Rev. B **69**, 115428 (2004).
[39] S. G. Chou, F. Plentz, J. Jiang, R. Saito, D. Nezich, H. B. Ribeiro, A. Jorio, M. A. Pimenta, G. G. Samsonidze, A. P. Santos, M. Zheng, G. B. Onoa, E. D. Semke, G. Dresselhaus, and M. S. Dresselhaus, Phys. Rev. Lett. **94**, 127402 (2005).
[40] A. Jorio, R. Saito, J. H. Hafner, C. M. Lieber, M. Hunter, T. M. McClure, G. Dresselhaus, and M. S. Dresselhaus, Phys. Rev. Lett. **86**, 1118 (2001).
[41] J. Jiang, R. Saito, G. G. Samsonidze, A. Jorio, S. G. Chou, G. Dresselhaus, and M. S. Dresselhaus, Phys. Rev. B **75**, 035407 (2007).
[42] Z. Jiang, E. A. Henriksen, L. C. Tung, Y.-J. Wang, M. E. Schwartz, M. Y. Han, P. Kim, and H. L. Stormer, Phys. Rev. Lett. **98**, 197403 (2007).
[43] R. S. Deacon, K.-C. Chuang, R. J. Nicholas, K.-S. Novoselov, and A. K. Geim, Phys. Rev. B **76**, 081406(R) (2007).
[44] K.-C. Chuang, R. S. Deacon, R. J. Nicholas, K.-S. Novoselov, and A. K. Geim, Philos. Trans. R. Soc. London, Ser. A **366**, 237 (2008).
[45] M. L. Sadowski, G. Martinez, M. Potemski, C. Berger, and W. A. deHeer, Phys. Rev. Lett. **97**, 266405 (2006).